

Amoxidation of 2-methyl pyrazine on supported ammonium salt of 12-molybdophosphoric acid catalysts: The influence of nature of support

KATABATHINI NARASIMHARAO^b, B HARI BABU^a, N LINGAIAH^a,
P S SAI PRASAD^{a,*} and SHAEEL A AL-THABAITI^b

^aInorganic and Physical Chemistry Division, Indian Institute of Chemical Technology, Hyderabad 500 007, India

^bDepartment of Chemistry, Faculty of Science, King Abdulaziz University, P. O. Box 80203, Jeddah 21589, Kingdom of Saudi Arabia
e-mail: saiprasad@iict.res.in

MS received 28 October 2013; revised 31 December 2013; accepted 2 January 2014

Abstract. Influence of the nature of support on the formation of catalytically active species was investigated to clarify the key factor for the synthesis of supported ammonium salt of 12-molybdophosphoric acid (AMPA) catalyst which maintains the activity of ammoxidation during 2-methylpyrazine reaction. With this aim, different loadings of niobia-, silica- and alumina-, supported AMPA catalysts were prepared. The AMPA loading was varied in the range of 5–25 wt%. The synthesized solids were characterized by nitrogen adsorption for BET surface area, XRD and ³¹P MAS NMR techniques. All the AMPA-supported samples are poorly crystalline even after 25 wt% AMPA loading. Investigations using ³¹P MAS NMR spectroscopy of samples revealed that Keggin ion existed as at least five different species on the supports. The investigated properties were acidity of the support and amount of AMPA loading on the support. Active sites for the ammoxidation of MP on supported AMPA catalysts seem to be the interacted and/or the lacunary species. Maximum catalytic activity could be obtained at lower loadings with AMPA deposited on acidic supports whereas the less acidic supports require higher loading. It was found that in order to efficiently generate the active interactive species, the support must have an acidity which promotes the formation of support-AMPA interactive species. It is possible to enhance the catalytic activity of the supported AMPA catalyst for ammoxidation of 2-methylpyrazine by controlling the acidity of the support and AMPA loading on the support.

Keywords. Ammonium salt of 12-molybdophosphoric acid; silica; niobia; alumina; ammoxidation of 2-methylpyrazine.

1. Introduction

Heteropolyacids (HPAs) with Keggin structure possess unique characteristics that make them very useful in catalysis; for instance, their highly acidic nature is very interesting in industrial reactions such as olefin hydration, alcohol dehydration, oxidation of hydrocarbons and methanol to hydrocarbons.^{1,2} The activity of Keggin type HPAs is attributed to their strong acidic and redox properties.³ However, in the acid form, they are highly soluble in many reactants causing difficulty in product separation. Their low thermal stability and surface area is also an impediment in vapour phase reactions. In general, HPAs can be made heterogeneous with high thermal stability and surface area by

supporting them on different inorganic oxides.^{4–7} Alternatively, HPAs can be transformed into fully or partially exchanged potassium, ammonium or cesium salts to improve their thermal stability as well as surface area. Hayashi and Moffat first reported that the ammonium salt of 12-molybdophosphoric acid (AMPA) was thermally stable with higher surface area and also a more efficient catalyst than the parent acid for the conversion of methanol to hydrocarbons.⁸ Subsequently, there were many efforts to correlate the physico-chemical properties of AMPA⁹ with its activity in reactions such as ethanol to hydrocarbons and oxidative dehydrogenation of isobutyric acid to methacrylic acid.

Vapour phase ammoxidation of 2-methylpyrazine (MP) to 2-cyanopyrazine (CP) is a simple route to synthesize amidopyrazine (popularly called pyrazinamide), which is an effective anti-tubercular drug.¹⁰ Forni *et al.*¹¹ and Bondareva *et al.*¹² found vanadium-based

*For correspondence

mixed oxide catalysts be active for the vapour phase ammoxidation of MP reaction. However, these catalysts required high reaction temperatures (close to 430°C), for this reaction which normally leads to thermal runaway since the highly exothermic oxidation of ammonia starts dominating under these conditions. In order to moderate the reaction conditions, Bondareva *et al.*¹³ employed vanadium-containing MPA as catalyst at lower reaction temperatures (380–390°C) and achieved about 75% CP yield. They reported the formation of AMPA in the catalysts after the reaction, even though the fresh catalysts were in the acid form. An American patent¹⁴ also proposed Mo-based phosphate catalytic system for achieving higher selectivity in ammoxidation of MP reaction. However, structural details of the catalyst were not disclosed in these cases. Therefore, it is interesting to study the structural aspects of AMPA which are responsible for the enhanced activity in ammoxidation reaction. It is known that catalytic functionality of the supported catalysts depends upon the nature and extent of surface species generated on the support surface.^{1,15} In the case of HPAs and their salts, the use of supports is believed to improve their stability and activity, as revealed by studies on silica and carbon supported HPA catalysts.^{16–23} However, in spite of the vast information generated, a clear picture has not evolved on the nature of surface species formed, in the case of supported AMPA catalysts.

In the present investigation, we have approached this problem by preparing supported AMPA catalysts using supports of different acidic properties and also varying the loading of AMPA. The catalysts were characterized by N₂ adsorption, XRD, FTIR and ³¹P MAS NMR spectroscopy. An effort has been made to identify the active species formed and correlate the formation of active species with the activity in ammoxidation of methyl pyrazine.

2. Experimental

2.1 Catalyst preparation

Bulk AMPA was prepared by dissolving ammonium heptamolybdate (SD Fine Chemicals, India, AR grade) and diammonium hydrogen orthophosphate (Loba Chemie, India, AR grade) in a minimum amount of water, in the stoichiometric ratio, maintaining pH at 2, followed by reflux at 100°C for 6 h and then concentrated on a water bath to reduce the initial solution to one-third of its initial volume. For the preparation of supported catalysts, the support (Nb₂O₅.nH₂O (CBMM,

Brazil), γ -Al₂O₃ (Harsha, AL-3996R) and SiO₂ (Ketjen fluid silica, F5) was initially taken in a flask and the deposition proceeded as described here. The amount of AMPA on the support was such that its composition varied in the range of 5–25 wt% in the finished catalyst. After drying at 120°C for 12 h, the catalysts were calcined at 400°C for 4 h in presence of air.

2.2 Characterization of catalysts

A conventional all-glass high vacuum system was used to determine the BET surface area of the samples, by nitrogen adsorption at liquid nitrogen temperature (−196°C). X-ray diffractograms of the catalysts were recorded on a Siemens D-5000 diffractometer using Ni filtered Cu K α radiation. Fourier transform infrared spectra of the samples were recorded on a Nicolet 740 FT-IR spectrometer under ambient conditions. Self-supporting discs containing the catalyst samples were prepared with KBr for recording the spectra.

³¹P MAS NMR spectra of the solids were recorded in a 400 MHz Varian spectrometer. A 4.5 s pulse (90°) was used with repetition time of 5 s between pulses in order to avoid saturation effects. The spinning rate was 5 KHz. All the measurements were carried out at room temperature using 85% H₃PO₄ as a standard external reference. Band resolution was carried out by treating the curves as Gaussian curves. The intensities and band widths were optimized to match the overall area under the curve with a mean deviation of +5%. The isokinetic point or the point of zero charge was estimated by potentiometric titration technique. NH₃TPD analysis was performed using CHEMBET 3000, Quantachrome, USA.

2.3 Activity measurements

Ammoxidation of MP was carried out in a fixed bed micro reactor made of pyrex glass (30 cm long) operating at atmospheric pressure. About 3 g catalyst, diluted with equal amount of quartz grains, was suspended between two quartz-wool plugs. The reactor was fitted with a concentric thermowell to house a thermocouple. It was placed inside an electrically heated split type furnace. An average particle size of 0.5 mm (18/25 BSS mesh) was chosen to eliminate mass transfer effects. The liquid reactant mixture (MP: H₂O = 1:2.5 v/v) was fed into the reactor using a microprocessor based syringe pump (B-Braun, Germany). A molar ratio of MP: water: ammonia: air of 1:13:7:38 was maintained

during evaluation of the catalysts. After the system attained equilibrium (in 1 h), at each temperature, product samples were collected and analysed by gas chromatography. Further details on the analysis are available elsewhere.^{24,25}

3. Results and discussion

3.1 N_2 gas adsorption

Among the supports, SiO_2 exhibited the highest BET surface area ($300\text{ m}^2/\text{g}$) followed by alumina ($196\text{ m}^2/\text{g}$) and hydrated niobia ($140\text{ m}^2/\text{g}$). A progressive decrease in surface area with the extent of loading was observed, as shown in table 1. This might be due to the greater mean pore diameter and pore volume of silica compared to that of the others. During preparation, solution transport into the pores of the support could have occurred by capillary action. It could also be due to refluxing of support with active phase solution under convective flow till the pores are filled up and then by diffusive mechanism, leading to partial obstruction of the support pores. Decrease in surface area is higher in silica-supported catalysts reflecting the difference in the salt support interaction. It is well-known that surface hydroxyl groups on metal support (M-OH) favour chemical interaction with the heteropolyacid/salt structure, though the mechanism is not yet clear.^{1,15}

3.2 Powder X-ray diffraction

The XRD patterns of fresh AMPA-supported silica catalysts calcined at 400°C are shown in figure 1A. The patterns of 5–10 wt% catalysts exhibited clear diffraction lines due to tridymite silica phase (JCPDS file No.14-260). On increasing loading to 15–20 wt%, intensity of the diffraction lines due to tridymite decreased substantially. No diffraction peaks

corresponding to AMPA were seen indicating that the AMPA was highly dispersed on the support surface.²⁶ At 25 wt% loading, however, the main diffraction peaks at $2\theta = 10.8^\circ, 15.2^\circ, 21.6^\circ, 26.5^\circ, 36.2^\circ$, etc. corresponding to AMPA (JCPDS file No.9-412) were observed. These results reveal that at lower loading, the AMPA is finely dispersed on silica surface. Only at 25 wt% loading, the catalyst attains crystallinity due to AMPA. These observations are in good agreement with those of Soled *et al.*²⁷ who also observed diffraction peaks of the ammonium salt of HPA beyond 30 wt% loading. Similar information was obtained from the XRD patterns of titania and zirconia supported AMPA catalysts.^{25,27,28}

Diffraction patterns of the fresh AMPA-supported niobia catalysts are shown in figure 1B. Niobia support²⁹ as well as 5–15 wt% AMPA-loaded catalysts existed in amorphous nature. As stated earlier, the AMPA might be highly dispersed on the support surface or present as fine crystallites with size less than 40 \AA that cannot be detected by XRD. The results are in good agreement with previous reports on MPA supported on different porous supports such as active carbon, and silica.^{30,31} At 20 wt% loading, the catalyst showed better crystallinity. This catalyst exhibited peaks due to MoO_3 along with those of AMPA. Upon increasing loading to 25 wt%, diffraction peaks due to AMPA were seen more clearly due to improved intensity when compared with those on 20 wt% sample.

The XRD patterns of fresh AMPA-supported alumina catalysts are shown in figure 1(C). The support exhibited broad peaks at $2\theta = 37.64^\circ, 45.90^\circ$ and 67.09° (JCPDS File No. 10-425), which corresponds to the gamma phase of Al_2O_3 . The XRD patterns of 5 and 10 wt% samples were similar to that of the pure support indicating fine dispersion of AMPA on the support. Upon increasing loading from 15 to 25 wt%, diffraction lines due to $AlPO_4 \cdot 2H_2O$ (JCPDS File No.15-274) and $NH_4AlP_2O_7$ (JCPDS File No. 31-39) appeared. Several

Table 1. BET surface area data of AMPA on different supports with different loadings.

Loading (wt%)	BET surface area (m^2/g)		
	SiO_2	Nb_2O_5 hydrated	$\gamma\text{-}Al_2O_3$
0	300	140	196
5	256	120	180
10	228	95	158
15	200	68	137
20	184	43	119
25	159	25	100

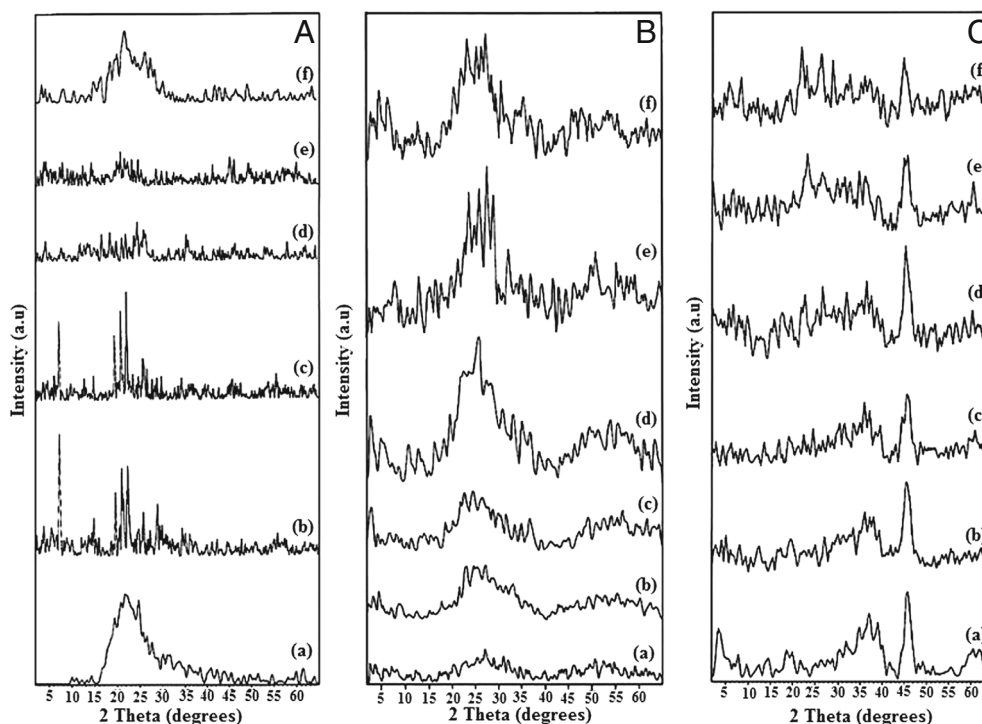


Figure 1. XRD patterns of (A) SiO_2 , (B) Nb_2O_5 and (C) $\gamma\text{-Al}_2\text{O}_3$ supported AMPA catalysts. (a) Pure support, (b) 5 wt%, (c) 10 wt%, (d) 15 wt%, (e) 20 wt% and (f) 25 wt%.

authors^{32,33} also reported formation of aluminum phosphate in the case of $\gamma\text{-Al}_2\text{O}_3$ -supported HPA catalysts. Increase in intensity of diffraction lines due to $\text{NH}_4\text{AlP}_2\text{O}_7$ with increase in loading was the main feature of the catalysts with higher loading. These results indicate that some part of aluminium phosphate formed at low temperature is converted into ammonium aluminium pyrophosphate during calcination.³⁴ Pyrophosphate formation might be low at lower loading due to low availability of ammonium and phosphate species to react with the support. A broad conclusion that can be made from the XRD data is that AMPA is highly dispersed at low loading and leads to formation of other compounds at higher loading. Only at 20–25 wt%, AMPA starts appearing in the XRD patterns.

3.3 Fourier transform infrared spectra

The FTIR spectra of silica and AMPA-supported silica catalysts are shown in figure 2A. The broad band at 3440 cm^{-1} is due to stretching vibration of H_2O molecules. Correspondingly, the IR band at 1632 cm^{-1} is due to bending vibration of H_2O molecules. The very strong and broad IR band at 1110 cm^{-1} with a shoulder at 1185 cm^{-1} could be assigned to the TO and LO modes of the Si-O-Si asymmetric stretching vibrations. The IR bands at 956 cm^{-1} and 800 cm^{-1} can be assigned to Si-O stretching and Si-O-Si symmetric

stretching vibrations, respectively and the band at 474 cm^{-1} is due to O-Si-O bending vibrations.³⁵ It is well-known that the unsupported AMPA reveals characteristic bands of $\text{PMo}_{12}\text{O}_{40}$ Keggin ion at 1060, 960, 860 and 790 cm^{-1} , corresponding to stretching vibrations of P-O_d , Mo-O_t , Mo-O_c -Mo, Mo-O_b -Mo (O_d -from PO_4 tetrahedral group, O_t -terminal groups from MoO_6 , O_b -bridge links resulting from the bond of corner-shared octahedral, O_c -bridge links resulting from the bond of edge-shared octahedral) of the Keggin unit and a band at 1410 cm^{-1} assigned to the stretching vibration of ammonium ion.³⁶ In the case of catalysts with 5–25 wt% AMPA loading, bands assigned to AMPA were very weak and were masked by strong absorption of silica in the region of the Keggin anion. It is noteworthy that intensity of the band at 962 cm^{-1} due to Si-O stretching vibration decreased with increase in AMPA loading from 5 to 10 wt% and this band completely vanished for 15, 20 and 25 wt% loaded samples. This disappearance of Si-O band might be due to the interaction of Keggin ion with Si-O functional groups during preparation of AMPA under acidic conditions. Another important feature of the FTIR spectra of SiO_2 -supported AMPA samples were the increasing broadness of the sharp band at 1110 cm^{-1} with increase in AMPA loading. Broadness might be a result of overlapping of bands due to Keggin ion. This observation clearly indicated the presence of Keggin ions.

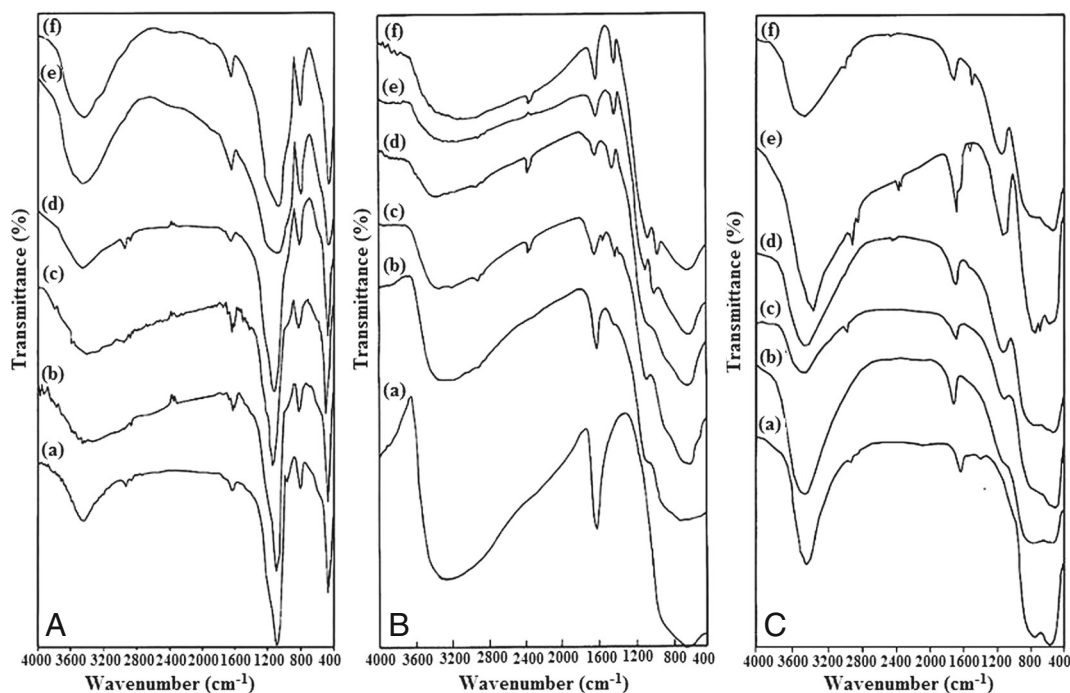


Figure 2. FTIR spectra of (A) SiO_2 , (B) Nb_2O_5 and (C) $\gamma\text{-Al}_2\text{O}_3$ supported AMPA catalysts. (a) Pure support, (b) 5 wt%, (c) 10 wt%, (d) 15 wt%, (e) 20 wt% and (f) 25 wt%.

Spectra of AMPA-supported niobia catalysts, with different loading are presented in figure 2B. FTIR spectrum of pure niobia showed an intense band at 1610 cm^{-1} , which corresponds, to the OH stretching vibration. A broad envelope could be seen in the spectrum in the region of $500\text{--}900\text{ cm}^{-1}$. In addition to the band at 1610 cm^{-1} , three bands with medium intensity were observed at 1410 , 1060 and 960 cm^{-1} in all niobia-supported AMPA catalysts. These bands being the characteristic bands of AMPA could be assigned to NH_4^+ , $\text{P}=\text{O}$, $\text{Mo}=\text{O}_t$ groups, respectively.¹³ The main feature of FTIR spectra of these catalysts was increase in intensity of all the bands upon increase in loading from 5 to 25 wt%. It is worth mentioning here that in the spectra of catalysts with low AMPA loading (5–15 wt%), bands corresponding to $\text{P}=\text{O}$ and $\text{Mo}=\text{O}$ were seen as broad humps. As reported by Concellon *et al.*¹⁸ MPA-supported niobia catalysts exhibited strong framework vibration bands of niobia below 900 cm^{-1} , overshadowing bands at 873 and 787 cm^{-1} of MPA and making interpretation of the bands based on the $\text{Mo}=\text{O}$ bond difficult. The bands appeared to become broader upon increasing MPA loading due to interaction of the acid with the support.³⁷ In the case of catalysts with higher loading (greater than 20 wt%), presence of bands corresponding to NH_4^+ , $\text{P}=\text{O}$ and $\text{Mo}=\text{O}$ were clearly seen revealing the presence of Keggin structure. Therefore, existence of AMPA is clearly confirmed which also corroborates the XRD data.

The FTIR spectra of the Al_2O_3 support and AMPA-supported alumina catalysts are shown in figure 2C. Alumina showed two broad envelopes at 560 and 750 cm^{-1} , respectively. Bands due to the support blocked the region where the three characteristic bands of Keggin ion normally appear.³² Other bands at 1060 cm^{-1} corresponding to $\text{P}=\text{O}_d$ and at 1410 cm^{-1} due to NH_4^+ stretching vibration provided information regarding the presence of Keggin species. However, caution must be exercised in interpreting the peaks as suggested by Rao *et al.*²¹ The authors demonstrated that IR spectroscopy may not be useful in concluding the state of heteropolyacids supported on alumina support, because they are not transparent to IR radiation in the range of $1000\text{--}700\text{ cm}^{-1}$. Increase in intensity as well as broadness of the two bands at 1410 and 1060 cm^{-1} were the main features of FTIR spectra of alumina-supported AMPA catalysts.

3.4 Solid state ^{31}P MAS NMR

NMR technique is known to be very sensitive to local chemical environment and surrounding symmetry of a given magnetic nucleus. Thus, it is important to use this technique to characterize changes in chemical environment after AMPA was supported on provided support. The ^{31}P MAS NMR spectrum of pure AMPA is shown in figure 3A. Fresh sample calcined at 400°C displayed two phosphorus resonance peaks, which indicates that

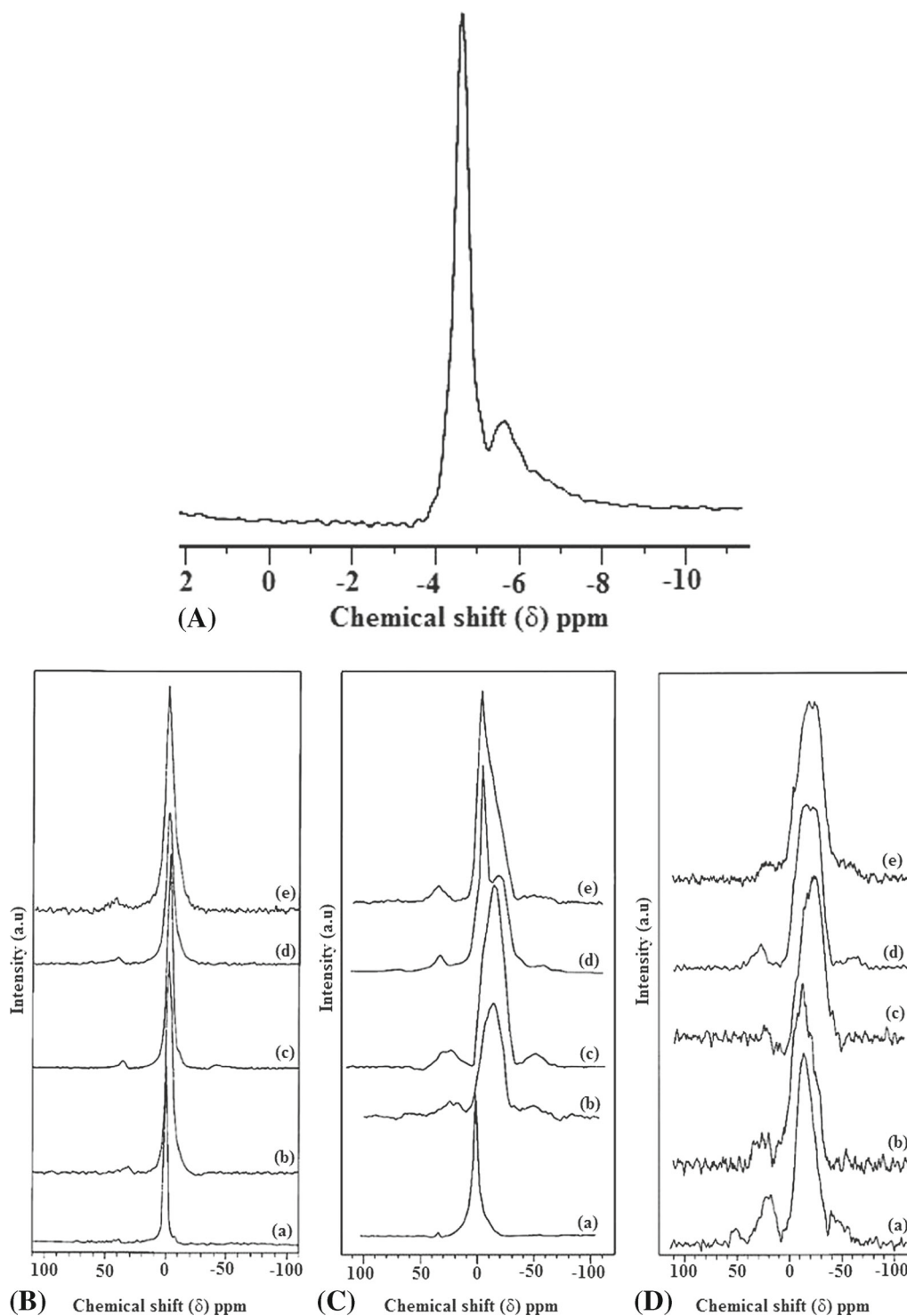


Figure 3. ^{31}P MAS NMR spectra of (A) AMPA catalyst calcined at 300°C and supported AMPA catalysts, (B) SiO_2 , (C) Nb_2O_5 , and (D) $\gamma\text{-Al}_2\text{O}_3$. (a) Pure support, (b) 5 wt%, (c) 10 wt%, (d) 15 wt%, (e) 20 wt% and (f) 25 wt%.

the catalyst exists in two different phases. A major sharp peak at -4.5 ppm and a small broad peak at -5.8 ppm were observed. It is well-known that ^{31}P NMR chemical shifts are greatly dependent on the number of water

molecules present in the sample. Therefore, the peaks -4.5 ppm and -5.8 ppm can be assigned to predominant P surrounded by Keggin units. Black *et al.*³⁸ while presenting ^{31}P anisotropies of different salts of

MPA showed that pure ammonium salt gives a peak at -4.5 ppm. Small peaks observed could be assigned to the P perturbed by hydrogen bonds of the four water molecules present as water of hydration.

When AMPA was impregnated on silica at 5 wt% (figure 3B), only a sharp single peak was observed at 0.0 ppm. On increasing the loading to 10 wt%, the peak moved up-field, i.e., -1.8 ppm but with enhanced bandwidth. Upon increasing the loading, i.e., to 15 wt%, it moved further up-field to -2.0 ppm with further increase in bandwidth. At 20 wt%, it moved to -2.2 ppm. At 25 wt% loading, the band shifted back to -1.4 ppm overlapped with low intensity broad band extending up to -12 ppm. These results indicate that with catalysts of low loading of AMPA on silica support, water molecules of hydration interact with silica support unperturbing the phosphate group of AMPA, which is intact within the Keggin cage. At higher loadings, the Keggin units also interact with silica support, which is reflected in the enhanced bandwidth. At 25 wt% the presence of the broad band near -12 ppm, in addition to the -1.4 ppm peak, clearly indicated that bulk AMPA interacted with the silica support and evidenced the presence of interacting species formed between them. These results are in line with the results obtained on MPA supported on silica by Damyanova *et al.*¹⁶ They studied the bulk as well as silica and zirconia-silica-supported MPA and by means of obtaining an intense and sharp line at $\delta = -4.2$ ppm concluded that bulk MPA exhibited a uniform phosphorous environment in a highly hydrated structure of the acid. The small peaks occurred due to different degrees of hydration. On calcination, below 350°C only dehydration takes place and above 350°C , the peaks became broad indicating decomposition of MPA. On silica support, even without heating, the peaks were split into several lines due to differently associated water molecules. The supported catalyst calcined at 550°C gave a broad peak indicating decomposition of the Keggin structure. Supporting MPA on zirconia-silica considerably broadened the signals. Vazquez *et al.*^{17,18} observed two peaks, one at -3.6 ppm and the other at -4.4 ppm on MPA-supported silica, the former due to non-interacted and the latter due to interacted species. Chang¹⁹ studied MPA-supported silica with different MPA loadings and observed three resonance peaks at 2.5, -3.6 and -10.0 ppm. They assigned -10.0 ppm peak to the species derived from the decomposition of MPA during calcination. The line at -3.6 ppm was assigned to pure MPA and the peak at 2.5 ppm was assigned to the interacting species with SiO_2 support. They also studied the effect of water and concluded that the

interacting species were more stable than pure crystalline MPA towards etching of water. Rene *et al.*²⁰ studied the spin-lattice relaxation of MPA-supported silica and concluded that the relaxation depends on the poly-anion: SiO_2 ratio for concentrations above that required for the saturation of adsorption sites on the silica surface. Rao *et al.*²¹ studied MPA-supported silica and observed a sharp peak at -3.8 ppm. Line width of the peak coincided with that of bulk MPA. These studies revealed that primary structure of the catalyst was only weakly perturbed on silica.

The ^{31}P MAS NMR spectra of AMPA-supported niobia catalysts are presented in figure 3C. The catalyst with 5 wt% AMPA showed a sharp single peak at -0.7 ppm. The peak at -0.7 ppm can be assigned to dehydrated Keggin species. Those with 10 wt% and 15 wt% AMPA showed single broad peaks with maxima at -13.4 and -16.5 ppm, respectively. The broad peak, in the present case, may correspond to $(\equiv\text{Nb-OH}_2)_n - [(\text{NH}_4)_{3-n}\text{Mo}_{12}\text{PO}_{40-n}]^{n-3}$ type of compound formed due to the interaction between hydroxyl groups on support surface ($\equiv\text{Nb-OH}$) and AMPA. Upon increasing AMPA loading to 20 wt%, the single broad peak was split into two peaks with a sharp signal at -2.2 ppm and another peak at -17.1 ppm. Even though, the magic angle spinning spectrum of AMPA consists of a single resonance chemical shift at -4.45 ppm, it is also known that upon calcination at higher temperatures, the chemical shift is moved to lower field because of dehydration. On further increase in the loading to 25 wt%, a single peak at -4.2 ppm was observed with enhanced band width. From these results, it is clear that at lower loading, the Keggin ion strongly interacts with support and on increasing the loading to 10–15 wt%, the samples show only interactive species. Upon further increase in loading, the catalysts seem to attain the bulk nature. Results are quite consistent with the results of XRD and FTIR.

Caliman *et al.*³⁹ studied the ^{31}P MAS NMR spectra of 12-tungstophosphoric acid supported on hydrated niobia. All the spectra showed two bands which means there are two kinds of chemical environments for $[\text{PW}_{12}\text{O}_{40}]^{3-}$; the first consists of bulky partially hydrated H_3PW crystals deposited on the niobia surface with weaker interactions and the second is anhydrous Keggin anion strongly and directly interacting with hydroxyl sites on the niobia surface which may be forming species such as $[\equiv\text{NbOH}_2]_n^+ [\text{H}_{3-n}\text{PW}_{12}\text{O}_{40}]^{n-3}$. Hydroxyl groups on the support surface can increase interaction among the Keggin anions and lead to larger aggregates on the surface without direct interaction with the support. A similar phenomenon can be expected in case of AMPA-supported niobia catalysts.

On alumina support, very up-field peaks were observed near -19 to -20 ppm (figure 3D), indicating decomposition of Keggin ion even at 5 wt% loading. Decomposition products could consist of a complex mixture of P_2O_5 and MoO_3 oxides and the peaks observed at different positions were due to the P_2O_5 – MoO_3 complexes with alumina. A detailed spectral data of AMPA on alumina catalysts are presented in table 2. The 5 and 10 wt% catalysts showed three peaks near -8 , -13 and -23 ppm. Iwamoto *et al.*⁴⁰ assigned the three peaks observed for MPA on alumina to monomeric phosphate, polyphosphate and $AlPO_4$, respectively and concluded that these ions were more stable and were adsorbed intact on alumina surface. Upon increasing the loading to 15–25 wt%, another peak near at -4.0 ppm was appeared. This peak might be due to bulk AMPA. The peak at -23.0 ppm could be assigned to pyrophosphate. Vazquez *et al.*¹⁷ reported that MPA-supported alumina showed two peaks at -3.3 and -10.8 ppm, the first one corresponding to the Keggin unit and the second one to the interacting species of MPA with the support. Rao *et al.*²¹ also observed two

broad peaks overlapping with each other at -9.5 ppm and -12.0 ppm with a line width of 1365 Hz. Cheng and Luthra³² studied MPA, $(NH_4)_6P_2Mo_{18}O_{62}$ and pentamolybdodiphosphate and showed that the phosphate group in $[PMo_{12}O_{40}]^{3-}$ and $[P_2Mo_{18}O_{62}]^{6-}$ was completely enclosed by a shell of MoO_6 octahedron and therefore shielded from the alumina surface.

Broad envelopes observed for AMPA on the supports seems to be composed of four to five peaks. The resolved band data are presented in table 2. With acidic supports, the ^{31}P chemical shift shifts to a small extent as observed with silica and niobia. In the case of alumina, which is less acidic than the other two supports, the shift is very much up-field. Intensities of the resolved bands, which vary with loading, give a good idea of the proportion of different species on the support surface. At loading up to an extent of 15 wt%, formation of associated species occurs due to interaction between support active groups and AMPA. As soon as the support surface is covered at higher loading, AMPA is observed in bulk phase.

Table 2. De-convoluted ^{31}P MAS NMR data of AMPA on different supports.

Loading (wt%)	SiO ₂	Nb ₂ O ₅	γ -Al ₂ O ₃
5%	3.44 (0.2)		-8.50 (4)
	0.00 (5)	4.30 (3.5)	-10.90 (3.5)
	-2.29 (4)	-0.71 (9.8)	-12.90 (3.5)
	-4.59 (11.5)	-5.30 (3.8)	-18.30 (5.5) -23.40 (2.8)
10%	1.00 (4)	1.20 (2)	4.70 (2.2)
	-5.00 (11.5)	-5.50 (8.8)	-3.50 (3.5)
	-11.0 (1.3)	-14.60 (9)	-8.13 (3.2)
		-21.80 (7)	-12.80 (6)
			-15.11 (2) -22.90 (4)
15%	3.77 (2)	-3.66 (3)	-4.70 (4.5)
	-0.94 (4.2)	-6.09 (3)	-12.90 (2)
	-4.70 (4)	-14.60 (5.5)	-14.11 (6)
	-13.20 (1.8)	-21.95 (7.6)	-20.00 (2) -22.80 (2.8)
20%	3.53 (1)		
	0.00 (3.7)		-4.50 (8)
	-2.65 (6)	-2.10 (11.2)	-12.60 (2)
	-5.30 (4)	-16.30 (6.4)	-23.20 (8.5)
	-8.84 (1)		
	-10.61 (1)		
25%	3.77 (2.3)		-4.32 (4.5)
	0.00 (3.5)	4.00 (2)	-10.50 (4)
	-2.83 (4.3)	0.00 (50)	-13.90 (3.7)
	-5.66 (3.5)	-6.00 (6)	-16.30 (3.2)
	-9.43 (2.8)	-12.00 (5)	-20.90 (3.2)
	-13.2 (1.5)	-20.00 (4.5)	-23.40 (4.2)

Broadening of ^{31}P NMR peaks of supported samples can be attributed to distortion of HPA symmetry compared to that in the crystalline form. This distortion is due to strong chemical interaction between the heteropolyanion and the support. It is known from literature related to the chemistry of supported HPAs that more or less strong interactions exist between the active phase and the support depending on the surface properties of the latter. Bruckman *et al.*³⁵ described in detail the interaction between HPAs and silica support. At low coverage (between 5 and 15 wt%), when the surface of the support is sparsely populated by Keggin units (KU), the system may consist of KU partially ‘immersed’ in the bi-dimensional hydration layer at the support surface. Bidimensional hydration layer provides a basic medium in comparison to strong acidic heteropolyacids. Thus, in conditions prevailing at the support surface, hydrolysis of Mo-O_c-Mo bonds (which link the triads of MoO₆ octahedra), takes place, resulting in the opening of the closed structure of the Keggin anion. Such transformations will result in formation of a flat structure composed of four triads linked together through the six Mo-O_c-Mo bridges and linked to the surface of silica through the PO₄ tetrahedron and some corner oxygen atoms of the triads. As a result of these chemical interactions between the heteropolyanion and the support (niobia, silica, zeolites and zirconia), it could be expected that acidity of the supported HPAs diminished and such systems will mainly show redox properties.

3.5 Activity for ammoxidation of 2-MP

Table 3 illustrates the values of point of zero charge (pzc) of the various supports used in this study. Pure supports offered low conversion of MP; a maximum of 20% in the case of niobia. Upon loading of 10 wt% AMPA in all supports, drastic increase in both the conversions of MP was observed. Highest conversion (95%) was observed in case of niobia-supported AMPA

catalyst compared to silica, and alumina-supported AMPA catalysts and alumina-supported AMPA catalyst showed lowest activity due to destabilization of Keggin structure on this support. Activity patterns obtained on different catalysts are shown in figure 4. Percentage conversion of MP obtained at a reaction temperature of 380°C was taken as a measure of activity. Catalysts prepared by impregnating AMPA on predominantly acidic supports reach maximum conversion at lower loading (such as AMPA on niobia and AMPA on silica reaching at 10 wt%) and that deposited on less acidic support such as alumina reached maximum conversion at a very high loading of 20 wt%. Therefore, it could be emphasized that acid–base property of the support plays a crucial role in fixing the maximum conversion attainable. The extent of formation of surface species on supported heteropolyacids depends on the extent of loading.^{26,41} In general, at low loading, acidity of the catalyst becomes weaker and less uniform than for the bulk solid due to formation of decomposition products.⁴² As the loading increases, acid strength increases.⁴³ The pzc of the support and the loading required to achieve maximum conversion seem to influence conversion.

It is necessary to understand as to how these parameters are interdependent. AMPA can interact with the support in various ways depending on the local acid–base environment and temperature at which it is activated before the reaction. Though it is difficult to explain with the limited information available from the existing results, some information can be inferred from published data on pH dependence of the stability of HPAs in solution. At pH 1.2, the acid or salt exists as [PMo₁₂O₄₀]³⁻ ion. At pH 2.2 of the solution, the Keggin ion loses one Mo-O group giving rise to [PMo₁₁O₃₉]⁷⁻ ion, and on further increase in pH to above 8, the complex ion degrades to [PO₄]³⁻ ion. In addition, HPAs when subjected to high temperature activation during preparation get dehydrated due to loss of surface as well as crystalline water. It is thus expected

Table 3. Ammonia TPD and catalytic activity data of AMPA on different supports.

S. No.	Support	Isoelectric point	Amount of desorbed NH ₃ (mmol/g)	AMPA loading at maximum activity (wt%)	Maximum conversion of MP (%) at 380°C
1.	Nb ₂ O ₅ · nH ₂ O	0.9	2.12 × 10 ⁻¹	–	20
				10	95
2.	SiO ₂	2.8	1.92 × 10 ⁻¹	–	15
				10	90
3.	γ-Al ₂ O ₃	7.2	1.10 × 10 ⁻²	–	18
				20	75

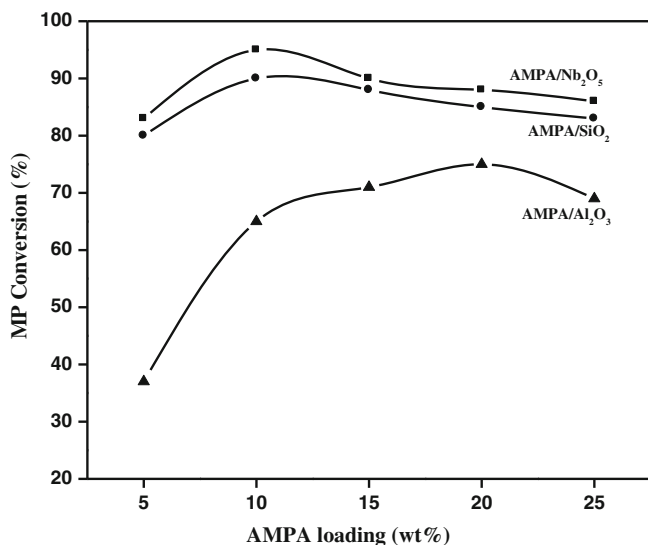


Figure 4. Conversion of 2-methylpyrazine over AMPA supported catalysts at different loadings at 380°C.

that some portion of AMPA may also exist as partially dehydrated species. Extending the same knowledge to the supported system of the present investigation, AMPA may exist as several species on the support. It may be construed that on acidic supports, the species exists as $(\equiv \text{M}-\text{OH}_2)^+ [\text{H}_{(3-n)}\text{PMo}_{12}\text{O}_{40}]^{n-3}$ or $(\equiv \text{M}-\text{O})_n- [\text{H}_{(3-n)}\text{PMo}_{12}\text{O}_{40}]$, thus retaining the Keggin structure. Further increase in pH may lead to loss of Mo-O group forming $[\text{PMo}_{11}\text{O}_{39}]^{7-}$ lacunary ions. AMPA when loaded on to the supports with a high pzc value (> 8), partial decomposition of the salt could occur. Different peaks in NMR spectra represent various species that formed on the supports.

Another important feature that can be observed from figure 4 is that the value of conversion of MP at maximum loading also decreases with increase in the pzc of the support. About 95% conversion could be achieved by 10 wt% AMPA on niobia whereas the value of maximum conversion progressively decreased to 75% in the case of 20 wt% AMPA on alumina. It appears that as the pzc value increases AMPA molecules are either converted into inactive species or are consumed in raising the net surface pzc to that required for active species formation.

3.6 Characterization of spent catalysts

FTIR spectra of 10 wt% AMPA-loaded niobia, silica and alumina supports after the reaction are shown in figure 5. Mostly there is not a major difference between the spectra of support before and after the reaction,

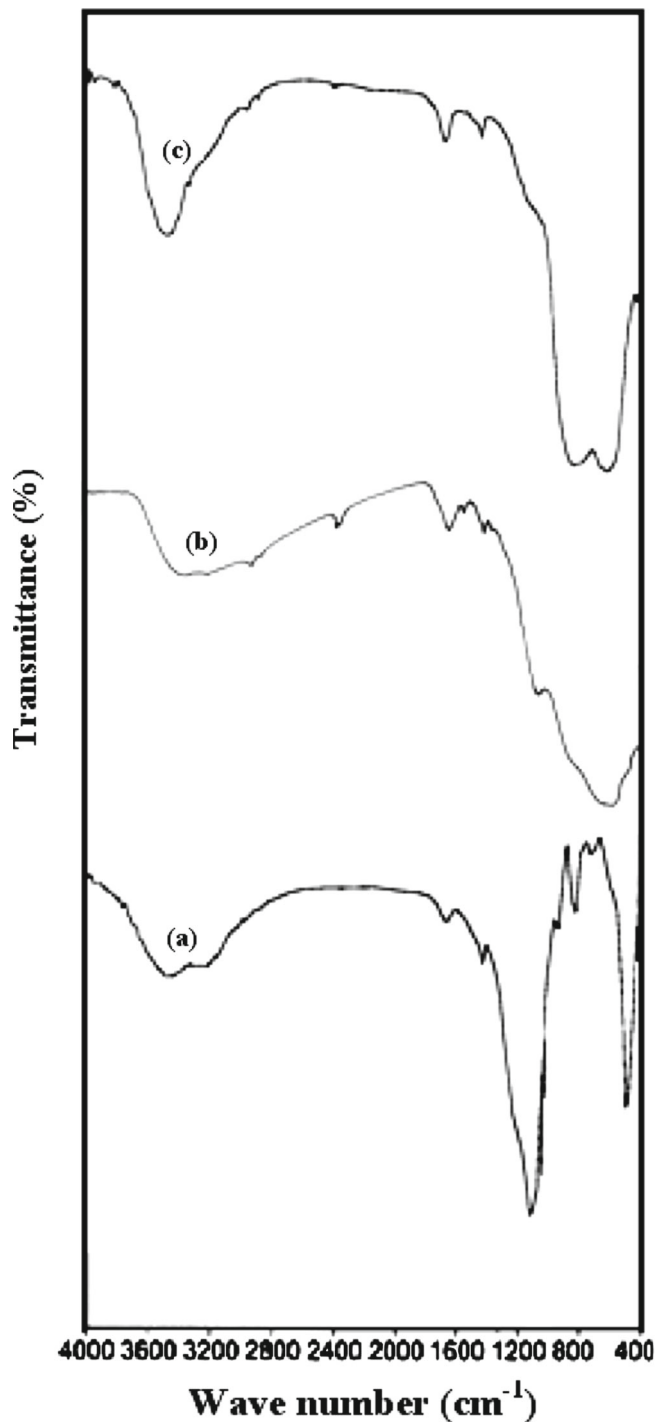


Figure 5. FTIR spectra of spent 10 wt% AMPA supported catalysts. (a) SiO₂, (b) Nb₂O₅ and (c) γ -Al₂O₃.

however, the used 10 wt% AMPA-loaded catalyst in silica and niobia showed one specific difference. Peaks due to Keggin ion were not overlapped by the support and the peak at 1410 cm^{-1} due to NH_4^+ stretching vibration is more intense in case of used catalyst; this is because the Keggin ion can be regenerated in presence of water. Catalysts in the present study exposed

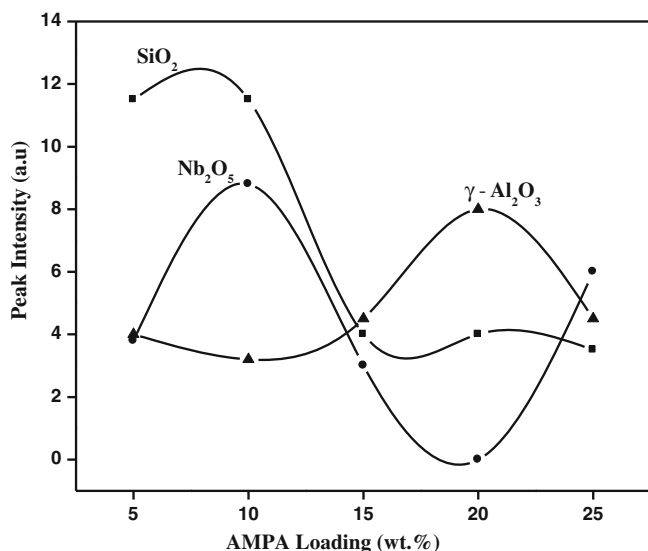


Figure 6. Effect of AMPA loading on the intensity of the ^{31}P MAS NMR peaks of the interacted species.

to ammonia and water (reactants in the ammoxidation reaction) for prolonged time is the reason for appearance of high intense peaks due to Keggin and NH_4^+ ions.

3.7 Correlation of catalytic activity and the active species as represented by the intensity of ^{31}P NMR bands

Possibilities of attaining several surface species have been delineated by ^{31}P MAS NMR spectroscopy. Bands assigned to interactive species formed on the surface of the support yield good information regarding activity of the catalyst on different supports. Activity in ammoxidation reaction of MP to CP which is presented in table 3 can be correlated to intensity of the peaks in the region of $-8 < \delta > -4$ ppm, which are due to the interactive and lacunary species formed on supported AMPA catalysts. Effect of AMPA loading on the intensity of these peaks of the interacted species is presented in figure 6. Niobia and silica showed maximum activity around 10 wt% loading, wherein maximum quantities of active species were present. For $\gamma\text{-Al}_2\text{O}_3$, the same is observed clearly at 20 wt%. Mestl *et al.*⁴⁴ in their partial oxidation studies using HPA catalyst have suggested that the intact Keggin anions are not the active species. From Raman spectroscopy studies it has been inferred that structurally reorganized intermediates are relevant for catalytic action. A similar explanation could be given to explain linear variation in the activity of the catalysts with the extent of structurally reorganized active species formed on the support.

4. Conclusions

In summary, influence of the nature of the support on formation of catalytically active species was investigated to clarify the key factor for the synthesis of supported AMPA catalyst which maintains the activity for ammoxidation of 2-methylpyrazine reaction. Active sites for ammoxidation of MP on supported AMPA catalysts seem to be the interacted and/or the lacunary species. Maximum catalytic activity can be obtained at lower loadings with AMPA deposited on acidic supports (niobia and silica), whereas less acidic supports (alumina) require higher loading. This is due to preferential formation of active species at a greater number on catalysts with acidic supports. Intensities of ^{31}P MAS NMR peak corresponding to these active species are well-correlated with ammoxidation activity.

Acknowledgements

The authors thank Dr. I Suryanarayana for his help in the spectroscopic analysis and BHB thanks Council of Scientific and Industrial Research (CSIR), New Delhi, India for financial support in the form of Senior Research Fellowship.

References

- Moffat J B 2001 *Metal–oxygen clusters: The surface and catalytic properties of heteropoly oxometalates*, New York: Kluwer Publications
- Haber J, Pamin K, Matachowski L, Napruszewska B and Połtowicz J 2002 *J. Catal.* **207** 296
- Misono M 2009 *Catal. Today* **144** 285
- Mallick S, Rana S and Parida K M 2012 *Ind. Eng. Chem. Res.* **51** 7859
- Parida K M and Mallick S 2008 *J. Mol. Catal. A: Chem.* **279** 104
- Rana S, Mallick S and Parida K M 2012 *J. Porous Mater.* **19** 397
- Mallik S, Dash S S, Parida K M and Mohapatra B K 2006 *J. Colloid Interface Sci.* **300** 237
- Hayashi H and Moffat J B 1982 *J. Catal.* **77** 473
- McMonagle J B and Moffat J B 1984 *J. Colloid Interface Sci.* **101** 479
- Rao K N, Gopinath R, Hussain A, Lingaiah N and Sai Prasad P S 2000 *Catal. Lett.* **68** 223
- Forni L, Oliva C and Rebuschini C 1988 *J. Chem. Soc. Faraday Trans.* **84** 2397
- Bondareva V M, Andrushkevich T V and Zenkovets G A 1997 *Kinet. Catal.* **38** 657
- Bondareva V M, Andrushkevich T V, Detusheva L G and Litvak G S 1996 *Catal. Lett.* **42** 113
- Lee Y K, Shin C H, Chang T S, Lee D K and Cho D H, inventors; Korea Research Institute of Chemical Technology, assignee. Process for preparing Cyanopyrazine. United States patent US 5,786,478. August 1995

15. Lopez-Salinas E, Hernandez-Cortez J G, Schifter L, Torres-Garcia E, Navarrete J, Gutierrez-Carrillo A, López T, Lottici P P and Bersani D 2000 *Appl. Catal. A: Gen.* **193** 215
16. Damyanova S, Fierro J L G, Sobrados I and Sanz J 1999 *Langmuir* **15** 469
17. Vazquez P G, Blanco M N and Caceres C V 1999 *Catal. Lett.* **60** 205
18. Concellon A, Vazquez P G, Blanco M N and Caceres C 1998 *J. Colloid Interface Sci.* **204** 256
19. Chang T 1995 *J. Chem. Soc. Faraday Trans.* **91** 375
20. Rene T, Deltcheff C R and Fournier M 1991 *J. Chem. Soc. Chem. Commun.* 1352
21. Rao K M, Gobetto R, Lannibello A and Zecchina A 1989 *J. Catal.* **119** 512
22. Moffat J B and Kasztelan S J 1988 *J. Catal.* **109** 206
23. Kaszletan S and Moffat J B 1987 *J. Catal.* **106** 512
24. Srilakshmi Ch, Rao K N, Lingaiah N, Suryanarayana I and Sai Prasad P S 2002 *Catal. Lett.* **83** 127
25. Rao K N, Gopinath R, Kumar M S, Suryanarayana I and Sai Prasad P S 2001 *Chem. Commun.* 2088
26. Kozhevnikov I V 1998 *Chem. Rev.* **98** 171
27. Soled S, Miseo S, McVicker G, Gates W E, Gutierrez A and Paes J 1997 *Catal. Today* **36** 441
28. Rao K N, Reddy K M, Lingaiah N, Suryanarayana I and Sai Prasad P S 2006 *Appl. Catal. A: Gen.* **300** 139
29. Tanabe K 1990 *Catal. Today* **8** 1
30. Sebulsky R T and Henke A M 1971 *Ind. Eng. Chem. Process Des. Dev* **10** 272
31. Izumi Y and Urabe K 1981 *Chem. Lett.* **10** 663
32. Cheng W C and Luthra N P 1988 *J. Catal.* **109** 163
33. Davydov A A and Goncharova O I 1993 *Russ. Chem. Rev.* **62** 105
34. Andrushkevich T V, Bondareva V M, Maksimovskaya R I, Popova G Y, Plyasova L M, Litvak G S and Ziborov A V 1994 *Stud. Surf. Sci. Catal.* **82** 837
35. Bruckman K, Che M, Haber J and Tatibouet J M 1994 *Catal. Lett.* **25** 225; (b) Bock J and Su G J 1970 *J. Am. Ceram. Soc.* **53** 69
36. Roach C M, Loronze N, Guillou N, Teze A and Herve G 2000 *Appl. Catal. A: Gen.* **199** 33; (b) Roach C M, Loronze N, Villanneau R, Guillou N, Teze A and Herve G 2000 *J. Catal.* **190** 173
37. Cubeiro M L, Damyanova S and Fierro J L G 1997 *Catal. Lett.* **49** 223; (b) Damyanova S, Gomez L M, Banares M A and Fierro J L G 2000 *Chem. Mater.* **12** 501
38. Black J B, Clayden N J, Gai P L, Scott J D, Serwicka E M and Goodenough J B 1987 *J. Catal.* **106** 1
39. Caliman E, Dias J. A, Dias S C L, Garcia F A C, de Macedo J L and Almeida L S 2010 *Micropor. Mesopor. Mater.* **132** 103
40. Iwamoto R, Fernandez C, Amoureux J P and Grimblot J 1998 *J. Phys. Chem. B* **102** 4342
41. Trolliet C, Condurier G and Vedrine J C 2001 *Top. Catal.* **15** 73
42. Bondareva V M, Andrushkevich T V, Paukshtis E A, Paukshtis N A, Budneva A A and Parmon V N 2007 *J. Mol. Catal. A: Chem.* **269** 240
43. Bachiller-Baeza B and Anderson J A 2004 *J. Catal.* **228** 225
44. Mestl G, Ilkenhans T, Spielbauer D, Dieterle M, Timpe O, Krohnert J, Jentoft F, Knozinger H and Schlogl R 2001 *Appl. Catal. A: Gen.* **210** 13